Distribution Agreement

In presenting this thesis or dissertation as a partial fulfillment of the requirements for an advanced degree from Emory University, I hereby grant to Emory University and its agents the non-exclusive license to archive, make accessible, and display my thesis or dissertation in whole or in part in all forms of media, now or hereafter known, including display on the world wide web. I understand that I may select some access restrictions as part of the online submission of this thesis or dissertation. I retain all ownership rights to the copyright of the thesis or dissertation. I also retain the right to use in future works (such as articles or books) all or part of this thesis or dissertation.

Signature:

_____ _____

Qingyang Xiao Date

Impact of Winter Heating on the Air Quality in China

By

Qingyang Xiao
Master of Public Health

Environmental Health

Yang Liu
Committee Chair

Paige E. Tolbert
Committee Member

Impact of Winter Heating on the Air Quality in China

By

Qingyang Xiao

B.A.
Peking University
2012

Thesis Committee Chair: Yang Liu, Ph.D.

An abstract of
A thesis submitted to the Faculty of the
Rollins School of Public Health of Emory University
in partial fulfillment of the requirements for the degree of
Master of Public Health
in Environmental Health
2014

Abstract

Impact of Winter Heating on the Air Quality in China
By Qingyang Xiao

China suffers from severe particulate matter (PM) pollution. Previous studies reported that the highest PM concentrations occur in winter. This high PM concentration is believed to be partly due to heating. This study used both remote sensing techniques and ground measured air pollutant concentrations to analyze the impact of heating on winter air quality through standard statistical tests and multivariate linear regression. Both the satellite retrieved data and ground measured air pollutant concentrations indicate that the air pollution levels increase significantly during the heating period. The average adjusted AOD ratio and the PM_{10} concentration ratio increase by 2.78 (p-value<0.01) and 0.33 (p-value<0.01) in the heating period, respectively. This increase in air pollution levels is significantly higher in the heating area than in the non-heating area. The increase in the adjusted AOD ratio and PM_{10} ratio is higher in the heating area than in the non-heating area by 2.19 (p-value<0.01) and 0.06 (p-value <0.01), respectively. Heating contribute significantly to the increase in the air pollution level in the heating period and the impact of heating on air pollution is immediate. The linear regression model indicates that heating demand, indicated by local temperature, can explain about 25% of the increase in air pollution levels during the heating seasons. Central heating has a pollution-control effect relative to individual heating. Our study furthers the understanding about spatiotemporal variability of PM pollution in China and provides information to make more effective pollution-control policies.

Length: The Abstract may not exceed one page, formatted according to the regular page formatting instructions (margins, spacing, font). The text itself cannot exceed 350 words (not counting the title etc.) The Abstract may be single-spaced.

Impact of Winter Heating on the Air Quality in China

By

Qingyang Xiao

B.A.
Peking University
2012

Thesis Committee Chair: Yang Liu, Ph.D.

A thesis submitted to the Faculty of the
Rollins School of Public Health of Emory University
in partial fulfillment of the requirements for the degree of
Master of Public Health
in Environmental Health
2014

Table of Contents

1 Introduction 1

1.1 $PM_{2.5}$ and its health impact 1

1.2 $PM_{2.5}$ in China 3

1.3 Central heating and its impact on winter air quality in China 4

1.4 Ground measurement of PM concentrations and its limitations 7

1.5 Remote sensing techniques and MODIS aerosol optical depth 7

1.6 Study objectives and hypotheses 9

2 Data and Methods 10

2.1 Study Area 11

2.2 Datasets and Processing 11

2.2.1 Remote Sensing Dataset 11

2.2.2 Ground Measured Air Pollutant Concentrations 13

2.2.3 Model simulated Data 16

2.2.4 Socioeconomic Data 17

2.2.5 Data Integration 18

2.4 Analytical Methods 20

3 Results 21

3.1 Descriptive Statistics 21

3.2 Spatiotemporal Variability of Adjusted AOD 23

3.3 T-test Results 25

3.4 Linear Regression Model 26

3.5 Spatiotemporal Variability of PM_{10} 28

3.6 Spatiotemporal Variability of $PM_{2.5}$ in 2013 30

4 Discussion 31

4.1 Spatiotemporal Variability of Air Pollution Levels 31

4.2 Impact of Heating and Other Possible Air Pollution Sources 33

4.3 Limitations and Future Study Directions 35

5 Conclusion 37

Acknowledgement 38

References 38

Tables and Figures 48

1 Introduction

1.1 $PM_{2.5}$ and its health impact

Particulate matter (PM) is a mixture of small solid and liquid particles which are suspended in the atmosphere. PM can be divided into different types based on their aerodynamic diameters. These include coarse particles (particles with an aerodynamic diameter of 10 microns or less), fine particles (particles with an aerodynamic diameter of 2.5 microns or less), and ultrafine particles (particles with an aerodynamic diameter less than 0.1 micron).

Previous epidemiological, physiological, and toxicological studies indicate that fine particles play a critical role in the negative health impact of PM pollution, because they contain complex chemicals and can be inhaled deeply into the lungs (Pope and Dockery 2006). Both rapid and sustained exposure to $PM_{2.5}$ are associated with adverse health outcomes, such as cardiovascular disease, respiratory disorders, immune disorder, and cancers (Pope and Dockery 2006; JZ Zhao et al. 2013; Brook et al. 2010; Vineis et al. 2006). Franklin et al. (2007) reported that an increase in the previous day's $PM_{2.5}$ concentrations by 10 $\mu g/m^3$ corresponded with a 1.12% (95% CI 0.29, 2.14%) increase in all-cause mortality and a 1.78% (95% CI 0.20, 3.36%) increase in respiratory related mortality in 27 U.S. communities. Pope et al. (2009) indicated that a 10 $\mu g/m^3$ decrease in $PM_{2.5}$ concentration was associated with a 0.61 ± 0.20 year increase in life expectancy in 211 U.S. counties. Kan et al. (2007)

estimated that a 10 μg/m^3 increase in the 2-day moving average $PM_{2.5}$ concentration was associated with a 0.36% (95% CI 0.11, 0.61%) increase in all-cause mortality and a 0.95% (95% CI 0.16, 1.73%) increase in respiratory related mortality in Shanghai, China. Thus, some studies suggested $PM_{2.5}$ as an indicator of particle pollution responsible for adverse health effects (Kan et al. 2007; Kappos et al. 2004; Bell et al. 2004).

Because previous studies described above provide strong epidemiological and toxicological evidence that PM exposure, especially fine particle exposure, has a significant association with negative health impacts, $PM_{2.5}$ has been regarded as an important ambient air pollutant and been controlled in the U.S. and in other countries. WHO Air Quality Guidelines suggest a 24-hour $PM_{2.5}$ concentration of 25 ug/m^3 (Organization 2006). In 2012, the U.S. Environmental Protection Agency (EPA) revised the annual $PM_{2.5}$ standard to 12 μg/m^3 and retained the 24-hour $PM_{2.5}$ standard of 35 μg/m^3 (MoEPo China 2013). In contrast, $PM_{2.5}$ was not listed as an ambient air pollutant by the Ministry of Environmental Protection of China until 2012. To improve air quality and public health protection, in 2012, the Ministry of Environmental Protection of China released the new ambient air quality standards, which included $PM_{2.5}$ and ozone as ambient air pollutants for the first time. These new ambient air quality standards, which will be applied in 2016, set the 24-hour

average $PM_{2.5}$ concentration at 75 μg/m^3 and the annual $PM_{2.5}$ concentration at 35 μg/m^3 (China 2012).

1.2 $PM_{2.5}$ in China

PM pollution in China has drawn broad concerns. Previous studies reported severe particulate pollution in China. Table 1 summarizes the results of previous measurements of $PM_{2.5}$ concentrations in China with at least a six-month monitoring period. The annual average of $PM_{2.5}$ concentrations ranged between 191μg/m^3 in Shijiazhuang and 30.3μg/m^3 in Taipei. The $PM_{2.5}$ concentrations showed largely spatial and temporal variability in China (Table 1). In all the cities aside from Tianjin, the highest $PM_{2.5}$ concentrations occurred in winter or spring, ranging between 34.5μg/m^3 in Taipei and 227.2μg/m^3 in Shijiazhuang, and the lowest $PM_{2.5}$ concentrations occurred in summer, ranging between 23.6μg/m^3 in Fuzhou and 146μg/m^3 in Shijiazhuang. Cao et al. (2007) measured $PM_{2.5}$ elemental carbon (EC) and organic carbon (OC) in 14 cities in China, and reported that the average EC concentrations in the 14 cities were 9.9μg/m^3 and 3.6μg/m^3 in winter and summer, and the corresponding OC were 38.1μg/m^3 and 13.8μg/m^3. Previous studies indicate that the high $PM_{2.5}$ concentrations in winter are partly due to winter heating (Cao et al. 2007; PS Zhao et al. 2013; He et al. 2001).

1.3 Central heating and its impact on winter air quality in China

Central heating systems are widely used in cities in Northern China, transferring hot water or steam to homes and offices for heating. Two sources of heat are used to heat water: waste heat from power plants, and combustion of coal, and, rarely, natural gas or oil, in the heating stations, which are built and operated by local governments. In 1955, China's central government divided the country into central-heating and non-central-heating areas using the Huai River and Qin Mountains (about 32 ℃N) as a natural way of separating them. Since then, it has provided funding support to local governments north of the Huai River and Qin Mountains in providing central heating (Huai-policy). The official heating period is decided by local governments based on the local temperature. When a city has five consecutive days with temperatures remaining at 5℃ or lower, the local government may start heating. Each year, from 15 October to 15 November, cities in the heating area start providing central heating, and, from 15 March to the end of April, those cities end their systematic heating. As local economies have developed, certain local governments in the southern non-heating area, such as in Wuhan, also provide central-heating for residents. Households in the areas where central heating is not available rely on individual heating, such as from heat-producing air conditioner units, electric space heaters, and domestic stoves, for household heating (Zhou et al. 2009).

Heating accounts for a large percentage of energy consumption in China. The building energy consumption (BEC) for heating accounted for 45% of the national urban building energy consumption (Cai et al. 2009). Coal is the main fuel used for heating. In 2003, more than 85 million tonnes of coal, 1 million tonnes of oil, and 1 billion cubic meters of gas were used for central heating in China, and the coal used for central heating alone accounted for more than five per cent of the total coal consumption in China (Committee 2004). The combustion of coal and other fossil fuels releases a large quantity of air pollutants, including PM. Chen et al. (2005) reported that the combustion of coal led to an estimated 290.24 Gg PM emission in 2000 in China. Previous studies analyzed the sources of $PM_{2.5}$ in Beijing and reported that coal combustion accounted for 19% of $PM_{2.5}$ on an annual basis, while in the heating season, this source accounted for as much as 37% of $PM_{2.5}$ (Song et al. 2006a; Song et al. 2006b). Zhang et al. (2013) monitored $PM_{2.5}$ in Beijing from 2009-2010, and reported that coal combustion account for 18% and 57% of $PM_{2.5}$ on an annual basis and in winter, respectively. Sustained exposure to this heating-caused severe particle pollution leads to negative health outcomes. Chen et al. (2013) analyzed the variability in total suspended particulates (TSP) concentration from 1981-2000 in China and reported that the ambient TSP concentrations were about 184$\mu g/m^3$ higher in Northern China than in Southern China due to the central heating policy. This high exposure to TSP may lead to a reduction in life expectancy at birth of about 5.5 years for residents in the north relative to those in the south.

Although previous studies indicate that central heating contributes to the severe air pollution in Northern China in winter and estimated the health impact of this winter air pollution(PS Zhao et al. 2013; Chen et al. 2013), these studies analyzed data from limited air monitoring stations in several major cities during a relatively short time period. The long-term analysis conducted by Chen et al. (2013), which indicates that a high TSP exposure in Northern China due to the central heating policy, has several limitations. First, they treated central heating as the only heating method adopted in Northern China; however, the central heating system is only accessible in cities and rural areas in Northern China have no access to the central heating system. For households in these areas, individual heating by stoves and electric heating instruments is widely used. Their methods of analysis cannot distinguish the impact of central heating from the impact of total heating and they assumed that all of the difference in the air pollution levels between Northern and Southern China were due to the central heating, which could be inaccurate. Second, they treated the Huai River and Qin Mountain as the boundary of the heating and non-heating areas; however, some municipalities that are located south of the Huai River have access to the central heating system. Thus, their definition of the central heating and non-central heating areas is incorrect. Third, they used TSP as the target air pollutant, which is a weak indicator of PM pollution related adverse health impact (Pope and Dockery 2006; Kan et al. 2007). Long-term and large-scale analysis of temporal and spatial variability of

$PM_{2.5}$ is needed to better understand particle pollution, its sources, and its impacts on public health in China.

1.4 Ground measurement of PM concentrations and its limitations

The continuous monitoring of PM_{10} in China began in 2000 in several central cities. There are currently 98 cities with PM_{10} monitoring stations in China and the historical daily air quality data of these cities can be tracked online. The monitoring of $PM_{2.5}$ began in 2012 and more than 100 cities have $PM_{2.5}$ monitoring stations currently. More monitoring stations in more cities are under construction. The hourly $PM_{2.5}$ concentrations are available online. One limitation of the ground monitoring of air quality is that the stations are distributed unevenly across the country, with most located in central cities (Figure 1) and the monitoring network not covering small cities or rural areas. Only 15% of the about 660 cities in the continental China were covered by the current air quality monitoring network. This limited spatial and temporal coverage of the ground measurement makes it difficult to conduct large-scale long-term analysis.

1.5 Remote sensing techniques and MODIS aerosol optical depth

Remote sensing techniques have become useful tools to estimate ground $PM_{2.5}$ concentrations, providing various spatial resolutions, acceptable accuracy, and a

chance to conduct large-scale analysis (Liu et al. 2012; Hu et al. 2013; Liu 2013). Aerosol optical depth (AOD) is a parameter widely used to estimate ground $PM_{2.5}$ concentrations through remote sensing techniques. Several satellite sensors provide various kinds of AOD measurements, with different algorithms, spatial resolutions and temporal resolutions. The Moderate Resolution Imaging Spectroradiometer (MODIS) instruments provide the most widely used aerosol products. Two identical MODIS instruments are onboard the NASA Earth Observing System (EOS) Terra and Aqua satellite, respectively. Terra passes from north to south across the study area at around 10:30am local time while Aqua passes from south to north across the study area at about 1:30pm local time. MODIS has 36 spectral bands, acquiring data in wavelength from 0.4 μm to 14.4 μm and providing information about atmospheric water vapor, surface temperature, land properties, and aerosol properties. Two algorithms are used to retrieve the AOD from MODIS data over land, the Dark-Target, which is used for dark land surface, and the Deep-Blue, which is used for bright ground. Previous studies reported acceptable accuracy of MODIS aerosol products in China (Hu et al. 2013; Song et al. 2009; Wang et al. 2007). By comparing the MODIS Terra retrieved AOD with ground-based AOD observation from the Chinese Sun Hazemeter Network (CSHN), Wang et al. obtained an annual mean correlation coefficient of 0.90 in China, ranging from 0.19 in Lanzhou to 0.94 in Yanting (Wang et al. 2007; Wang et al. 2010). Liu et al. (2012) reported that both Terra and Aqua

AOD in Beijing are highly related to the ground measured values reported by AERONET, with a correlation coefficient around 0.9.

AOD is considered as a strong indicator of surface $PM_{2.5}$ levels together with other information, such as meteorological factors and land use (Liu 2013). Tsai et al. (2011) reported that the correlation coefficient of relative humidity and boundary layer height normalized AOD and ground $PM_{2.5}$ concentrations was about 0.68 in Taiwan. Thus, it is possible to use the satellite-retrieved data to reflect ground air pollution levels and analyze the temporal and spatial variability of air pollution.

1.6 Study objectives and hypotheses

The objective of this study is to analyze the impact of winter heating on particulate pollution in China through both remote sensing techniques and ground measurement. First, standard statistical tests were conducted to examine the spatiotemporal variability of adjusted AOD in China. Then we developed a multivariate linear regression model with temperature and population normalized central heating area as independent variables, and increase of the adjusted AOD ratio during the heating period as dependent variables to explain the spatial difference of adjusted AOD increase between the heating and non-heating seasons in each municipality. The statistical significance of each predictor was analyzed to estimate its impact on winter air pollution. Ground measured PM_{10} concentrations estimated from daily Air

Pollution Index (API) and ground measured hourly $PM_{2.5}$ concentrations were also analyzed to describe the spatiotemporal variability of ground air pollution in China and support the results of adjusted AOD analysis.

The hypotheses of this study are:

1. H_0: Particulate matter concentrations stay the same during the heating and non-heating periods;

   H_A: Particulate matter concentrations increase significantly during the heating period;
2. H_0: Heating has no significant impact on winter air pollution in China;

   H_A: Heating has a significant impact on winter air pollution in China; and
3. H_0: Central heating has the same impact as individual heating on air pollution level;

   H_A: Central heating releases less air pollution relative to individual heating.

2 Data and Methods

The datasets used in this study consist of remote sensing data, ground measured air pollutant concentrations, model simulated data, and socioeconomic data. The main analytical methods employed in this study include a standard statistical test and multivariate linear regression model.

2.1 Study Area

The study area of this analysis is mainland China, excluding Tibet, Xinjiang, and Qinghai provinces (Figure 1). Tibet and Qinghai provinces were excluded because they are located on the Qinghai-Tibet Plateau and the low local temperature due to high latitude requires year-round household heating. Xinjiang province was excluded because its deserts are major natural sources of particulate matters. In addition, their bright surfaces also make high-quality satellite AOD retrieval very difficult.

2.2 Datasets and Processing

2.2.1 Remote Sensing Dataset

The Collection 5 level 3 MODIS AOD product at 550 nm from the Terra satellite (MOD08_D3, "Optical_Depth_Land_And_Ocean_Mean") over China area (Figure 1) were obtained from the Goddard Space Flight Center (http://ladsweb.nascom.nasa.gov/data). The level 3 AOD product (1 °×1 °spatial resolution) is a global aggregation of MODIS level 2 Dark-Target AOD product (10 km spatial resolution) (Hubanks et al. 2008). The "QA" parameter of the level 2 product provides information about quality of the retrieved data, ranging from 0 (no confidence or fill) to 3 (very good confidence) (Hubanks et al. 2008). All pixels from level 2 AOD product with quality flag=1, 2, and 3 are used and gave equal weight to drive the level 3 product (Hubanks et al. 2008; Ruiz-Arias et al. 2013). Standard deviation derived from the level 2 pixels is also provided. Ruiz-Arias et al. (2013)

calibrated the validation of Terra level 3 AOD product with ground AERONET stations globally and reported that the error of this product was 0.03 ± 0.14. Operational Terra level 3 AOD data over China area (Figure 1) from 2003 to 2010 were obtained and processed.

The quality of MODIS level 3 data was controlled by the coefficient of variability (CV), which is the AOD value divided by the standard deviation of AOD. Only pixels with CV equal to or less than 20 were included in this analysis. There are some missing data in the MODIS level 3 dataset due to snow cover and cloud cover. The missing data is distributed un-evenly across the study area; the northern part has more missing data than the southern part. To control the quality of the satellite dataset, two datasets were used for further analysis. One dataset includes all available pixels (full dataset), and another dataset includes all the pixels with at least one valid level 3 AOD value per month (one-obs-per-month dataset).

The AOD was normalized by absolute humidity and PBL (Equation 1) during the satellite passing time (Dawson et al. 2007; Alfoldy et al. 2007) because previous studies indicated that the correlation between AOD and PM was improved if AOD is normalized by daily absolute humidity and PBL (Tsai et al. 2011; Koelemeijer et al. 2006). The absolute humidity was calculated from relative humidity and temperature in the corresponding time period from the GEOS-Chem dataset (Equation 2). The

adjusted AOD was used to describe the spatiotemporal variability of air pollution level in section 3.2.

$$\text{Adjusted} - \text{AOD} = \text{AOD}/(\text{AH} \times \text{PBL}) \quad \text{Equation 1}$$

$$\text{AH} = 6.112 \times e^{(17.67 \times \text{T})/(\text{T}+243.5)} \times 2.1674 \times \text{RH}/(273.15 + \text{T}) \quad \text{Equation 2}$$

Where AH=absolute humidity (g/m^3) during satellite passing time; T= temperature (℃) during satellite passing time; RH=relative humidity during satellite passing time; PBL= planetary boundary layer thickness (km).

To eliminate the interannual variability, the adjusted AOD ratio, which is the average adjusted AOD divided by the annual adjusted AOD, was used in the statistical test and multivariate linear regression.

2.2.2 Ground Measured Air Pollutant Concentrations

The daily PM_{10} concentration was derived from the daily API data. The daily API of each municipality was issued by the Ministry of Environmental Protection of the People's Republic of China from 2003-2012 and are available online at the Data Center website (http://datacenter.mep.gov.cn/). The API is derived by ground measured concentrations of three ambient air pollutants: SO_2, NO_2, and PM_{10}. The API consists of two major parameters: the primary pollutant and the API value. The individual API value of each of the three air pollutant is calculated by range-based-linear-regression separately, and the air pollutant with the highest

individual API value is reported as the primary air pollutant. Its individual API value is reported as the API value of the day. If the API value is lower than 50, the air quality will be reported as "Good" and no major air pollutant will be reported (Gong et al. 2007; Choi et al. 2008). Seventy-six municipalities in the study area with at least 2 years API records and at least 200 valid API records in each year were included in this study.

The PM_{10} concentrations derived from the daily API record were used by previous studies to conduct temporal and spatial analysis (Song et al. 2009; Gong et al. 2007; Choi et al. 2008). In the API dataset, PM_{10} polluted days, other air pollutant polluted days and good air quality days account for 76%, 4%, and 20% of the total city-days, respectively. To estimate the PM_{10} concentrations from the daily-reported API, the following strategies were used: for PM_{10} polluted days or good air quality days, the PM_{10} concentration was estimated by range-based-linear-regression (Equation 3) (Song et al. 2009; Choi et al. 2008). For other air pollutant polluted days, triangular distribution was used to estimate the PM_{10} individual API from the reported API. The distribution is described in Equation 4 and it is based on the assumption that the three air pollutant concentrations vary consistently.

$$C_{PM\,10} = \frac{C_{high} - C_{low}}{I_{high} - I_{low}} \times \left(I_{PM\,10} - I_{low}\right) + C_{low} \qquad \text{Equation 3}$$

$$I_{PM\,10} = I_{reported} \times f(x) \qquad \text{Equation 4}$$

Where $C_{PM\,10}$=PM_{10} concentration (mg/m^3); C_{high}=the highest limitation of PM_{10} concentration in the corresponding PM_{10} range (mg/m^3); C_{low}=the lowest limitation of PM_{10} concentration in the corresponding PM_{10} range (mg/m^3); $I_{PM\,10}$=the individual API of PM_{10}; I_{high}=the highest limitation of PM_{10}'s individual API in the corresponding API range; I_{low}=the lowest limitation of PM_{10}'s individual API in the corresponding API range; $f(x)$=the random number from the triangular distribution with the following probability density function: $\int(x) = 2x$

The monitoring of ground $PM_{2.5}$ began in some major cities in December, 2012 in China (data are available online at the $PM_{2.5}$ monitoring website (http://www.cnpm25.cn)). Each city has 7-8 monitoring stations, on average, which are operated by the local environmental protection agency. The hourly $PM_{2.5}$ concentrations, measured by the gravimetric method, are reported online. Hourly $PM_{2.5}$ data in 2013 of 109 municipalities in the study area were used in this study. The daily $PM_{2.5}$ data were averaged from the hourly $PM_{2.5}$ from each monitoring stations. The daily city-level average $PM_{2.5}$ concentrations were averaged from the daily $PM_{2.5}$ data from all air quality monitoring stations in each city.

The daily PM concentrations were used to describe the spatiotemporal variability of air pollution level in section 3.5 and 3.6. To eliminate the between annual variability, the $PM_{2.5}$ and PM_{10} concentrations ratio, which is the average PM concentrations

divided by the corresponding annual PM concentration, was used in the two sample t-test.

2.2.3 Model simulated Data

The LandScan Population Project produces ambient population distribution globally at 30 ´´(approximately 1 km) spatial resolution through spatial data, imagery analysis technologies, and a multi-dimensional asymmetric modeling approach. Previous validations reported that in Germany, Israel, and the Southwest U.S. the simulated LandScan population has less than 10% difference compared with the totals of the official census in all the study areas in 1998 (Dobson et al. 2000). The yearly LandScan data over the study area from 2003 to 2010 were obtained from the Oak Ridge National Laboratory website (http://web.ornl.gov/sci/landscan).

Goddard Earth Observing System Model, Version 5 (GEOS-5) was produced by the NASA Global Modeling and Assimilation Office (GMAO). GEOS-5 data at 2 ° latitude by 2.5 °longitude spatial resolution, and 3-hour temporal resolution were used in this study to provide meteorological information, such as temperature, relative humidity, and planetary boundary layer thickness (PBL) within 3 sigma vertical layers. Local temperature at 11:00 am local time, around the satellite passing time, was obtained to normalize AOD. Daily temperature were calculated and used as a parameter in the linear regression model was. To analyze the impact of temperature

on air pollution level spatially and temporally, two temperature variables were processed. The spatial temperature is the average of temperature during the heating period from 2003-2010, which reflect the spatial distribution of temperature. The interannual temperature is the average temperature in the heating period of each year minus the spatial temperature, which reflects the interannual variability of temperature.

2.2.4 Socioeconomic Data

The socioeconomic parameters used in this analysis, including size of the central heating area and thermal power generation, were obtained from the China Statistical Yearbook and the China Electric Power Yearbook. The China Statistical Yearbook, which is compiled by the National Bureau of Statistics of China and published by the China Statistics Press, is an annual statistical publication summarizing the social-economic data of China. The province-level size of central heating area data from 2003 to 2010 were obtained from the China Statistical Yearbook from 2004 to 2011. The municipality-level data were estimate from the province-level data using by the population of each municipality as weight. The China Electric Power Yearbook, which is compiled by the "China Electric Power Yearbook" Editorial Committee and published by the China Electric Power Press, is an annual summary of the development, achievements, policies and events of China's power sector. The province-level by-type electricity production data from 2003-2010 were from the

section of statistical data of the China Electric Power Yearbook. The year 2003 and 2005 don't have the by-type electricity generation data, so the thermal power generation of the two years were estimated from the total electricity generation data and the average percentage of thermal power over the total of the other six years.

2.2.5 Data Integration

Municipality is the unit for analysis in this study and all the data were averaged and assigned to municipality based on their location using the nearest neighbor approach through ArcGIS 10.1. There were a total of 294 municipalities in the study region, whose average area was 2.03×10^4 km^2. MODIS level 3 data were averaged from pixels in each municipality. Adjusted AOD values for municipalities with no pixel within it were estimated by the value of the nearest pixel, which was less than one degree away from the boundary of the municipality. Adjusted AOD values of municipalities with no pixel within it and the nearest pixel was more than one degree away from it were recorded as missing. The total population of each municipality was estimated as the sum of the LandScan pixels located within each municipality. Population density was calculated as the total population divided by the corresponding area of each municipality. The temperature data were averaged from the GEOS-5 pixels within each municipality. Temperature data of municipalities with no pixels within it were estimated by the value of the nearest pixel. The municipality-level socioeconomic data were derived from the province-level data

from the yearbook, weighted by the population of each municipality. Size of central heating area indicates municipalities' ability to provide central heating. In this analysis, the size of central heating area was normalized by the local population ($km^2/10^4$ person) and this parameter was used to reflect the personal central heating source. If the total heating demands are held constant, the higher the normalized central heating area, the larger proportion of heating demands are met by central heating, and the fewer individual heating activities are conducted. This parameter was used in the linear regression model to analyze the impact of central heating relative to other heating activities.

To analyze the impact of heating, we divided each year into heating and non-heating periods, and we divided the whole study region into heating and non-heating areas. In this study, we set the heating period from November 16 in each year to February 28/29 in the next year, and the non-heating period from May 1 to October 14. Because the central heating start date varies in different areas and in different years, we exclude the dates from October 15, when the municipalities located in the furthest north region of China start central heating, to November 15, when the municipalities located near the southern boundary of the heating area start central heating. March and April were also excluded from the analysis because the frequent sand storms in spring contribute substantially to PM levels (Zhang et al. 2006). We normalized the parameter of air pollution level (adjusted AOD value, PM_{10} concentration) for each

municipality by the annual mean of the municipality to eliminate the impact of interannual variability and the spatial difference in the baseline pollution level. By eliminating the interannual variability, we can pool data from different years together to get a larger sample size. The spatial difference in the baseline pollution level reflects impact of temporal-constant emission sources, such as emission from industry and transportation. By eliminating the spatial difference in the baseline pollution level, we can avoid the effect of temporal-constant emission sources and emphases on the temporal emission sources, such as winter heating. We set the heating area as municipalities with the central heating area more than zero km^2, while the non-heating area as municipalities with zero km^2 central heating area. The heating and non-heating area may vary from year to year, because some provinces may begin or stop central heating during the study period.

2.4 Analytical Methods

Two sample t-tests were conducted to compare the air pollution level (adjusted AOD ratio, $PM_{2.5}$ concentration ratio, and PM_{10} concentration ratio) of each municipality during heating and non-heating periods. Data of these eight years were pooled together. The hypotheses 1 and 2 described in section 1.6 were tested by the t-test using both satellite retrieved data and ground measured data.

Then, we developed a municipality-level linear regression model to explain the spatial difference of the elevated air pollution level in the heating period. The model structure can be expressed as follows:

$$AOD_{adj} = \beta_0 + \beta_1 \times Temp_{Interannual} + \beta_2 \times Temp_{Spatial} + \beta_3 \times Heating + \beta_4 \times Temp_{Interannual} \times Heating + \beta_5 \times Temp_{Spatial} \times Heating \quad \text{Equation 5}$$

Where AOD_{adj} = adjusted AOD; $Temp_{Interannual}$ = interannual temperature; $Temp_{Spatial}$ = spatial temperature; Heating = population normalized size of central heating area.

The statistical significance of each independent variable was analyzed to estimate the impact of heating demands, which is indicated by the temperature parameters, and central heating on winter air pollution in China. We also considered other predictors, such as electricity generation and population density; however, preliminary results indicated that these variables were not statistically significant; thus, we removed them from the final model.

3 Results

3.1 Descriptive Statistics

The summary statistics of the two datasets properties are presented in Table 2. The mean of adjusted AOD of the full dataset (0.18) is slightly lower than that of the one-obs-per-month dataset (0.19), because the full dataset has more missing data in the heating period. In contrast, the difference in the adjusted AOD between the

heating and non-heating periods and the difference in the adjusted AOD ratio between the heating and non-heating periods of the full dataset are higher than those of the one-obs-per-month dataset. This could be the reason the full dataset includes more pixels in Northern China, which may have a larger increase of air pollution levels in the heating period than those in Southern China (Figure 2). The one-obs-per-month dataset has about 24% fewer pixel-years compared to the full dataset.

The histograms of parameters are illustrated in Figure 3, which shows that the dependent variable, the change of adjusted AOD ratio, of the two datasets are approximately normally distributed. The two temperature parameters are approximately symmetrically distributed, while the distribution of normalized central heating area is highly right skewed. The normalized central heating area relates to both the Huai-policy and local development. Municipalities which are located in north of the Qin Mountain and Huai River, and whose economies are well developed have the highest normalized central heating area value. Table 2 shows that the municipality-level adjusted AOD ratio difference between heating and non-heating periods in the full dataset and the one-obs-per-month dataset is 2.32 and 1.73, respectively. The average interannual temperature and spatial temperature is 0 ± 1.17 and 3.76 ± 7.96 degree centigrade, respectively. The spatial temperature shows larger variability than the interannual temperature does. The large variability of the spatial

temperature relates with the large range of latitude and complex geographical environment of China, while the interannual temperature keeps relatively stable.

3.2 Spatiotemporal Variability of Adjusted AOD

To analyze the air pollution levels, average adjusted AOD data of each municipality in the study area during the study period were divided into four spatiotemporal groups: in the heating area during heating period (HH), in the heating area during non-heating period (HN), in the non-heating area during heating period (NH), and in the non-heating area during non-heating period (NN). The yearly average adjusted AOD of each spatiotemporal group together with the average annual adjusted AOD over the whole study region (All) from 2003-2010 are shown in Figure 4. The average annual adjusted AOD over the whole study region slightly increased from 0.17 in 2003 to 0.23 in 2010, with an increasing rate less than 0.01/year. However, the average adjusted AOD in the heating area during heating period increased almost twice from 0.48 in 2003 to 0.85 in 2010, with an increasing rate of 0.07/year. There is a dip of average adjusted AOD in the HH group from 2009 to2010. Because we didn't show adjusted AOD data after 2010, this dip could be interannual variability rather than indicating a constant trend. The average adjusted AOD value in the heating area during the heating period is always the highest among these spatiotemporal groups, and the average adjusted AOD values during heating period are always higher than the corresponding values during non-heating period, both in the heating and

non-heating areas, with an average difference of 0.40. The average difference in the adjusted AOD between heating and non-heating periods in the heating area was 0.66, which was much higher than that in the non-heating area (0.14).

The spatial distribution of the annual adjusted AOD from 2003-2010 is shown in Figure 5. The highest annual adjusted AOD values occur in Hebei, Henan, Shandong, and Gansu provinces, while the lowest values occur in the furthest north region (Heilongjiang province and part of Inner Mongolia) and south China (Hainan, Yunnan, Guangdong, and Fujian provinces). This spatial pattern was stable from 2003-2010, and the annual adjusted AOD values increased in some areas during these eight years. The temporal trends vary over China. The regions with the highest adjusted AOD also show a largest increase of the annual adjusted AOD, while the annual adjusted AOD in Southern China remains the same during these eight years.

Figure 6 shows the distribution of the average adjusted AOD in heating and non-heating period from 2003-2010. Though the average adjusted AOD in the heating period in some areas in Southern China, such as Yunnan, Fujian and Hainan provinces, were similar as those in the non-heating period; however, in most areas, both in the heating and non-heating areas, the average adjusted AOD during heating period were much higher than those in the non-heating period. Paired t-test indicates that the average adjusted AOD increases significantly by 0.43 during the heating

period (p-value<0.01). The highest increase of adjusted AOD in the heating period occurs in the Inner Mongolia, Hebei, Henan, and Shandong provinces.

3.3 T-test Results

To statistically compare the difference of air pollution level between the heating and non-heating periods in the heating and non-heating areas, several two sample t-tests were conducted on the adjusted AOD ratio. Adjusted AOD ratio, rather than the absolute value of AOD, is used in the analysis. Thus, the innterannual variability will not affect the comparison within each year and the increase of adjusted AOD rather than the annual average value will be emphasized. The heating and non-heating periods were divided as described previously. Two different datasets were analyzed to control the data quality: one dataset includes all available satellite pixels (full dataset), the other dataset includes satellite pixels with at least one valid observation per month (one-obs-per-month dataset). The summary statistics of these two datasets is shown in Table 2.

We first compared the values of adjusted AOD ratio between heating and non-heating periods with the eight-year data pooled together. The t-test results indicate that there is a significant increase in the adjusted AOD ratio during the heating period in China, and the estimated difference is 2.30 and 1.72 in the full dataset and the one-obs-per-month dataset, respectively (p-value<0.001, Table 3). To analyze the

immediate impact of heating on the air pollution level, we also compared the adjusted AOD ratio in October 1-14, the two weeks before the central heating starts, and in November 16-30, the two weeks after the central heating starts. The difference in the monthly AOD ratios in these two months is 1.36 and 1.11 in the full dataset and the one-obe-per-month dataset, respectively (p-value<0.001). This difference is relatively small compared with the difference in adjusted AOD ratio between the heating and non-heating periods, because at the beginning of the heating period, the temperature is relatively high and the heating demands is relatively low. Thus, the air pollution emission due to heating activities is relatively low. We then analyzed the spatial difference of the change of adjusted AOD in the heating period. We calculated and compared the change of the AOD ratio in the heating period in the heating and non-heating areas. The t-test results indicate that there was a significant spatial difference in the increase of air pollution levels during the heating period. The increase of the AOD ratio in the heating area was higher than in the non-heating area by about 1.44 and 0.94 in the full dataset and one-obs-per-month dataset, respectively (Table 3).

3.4 Linear Regression Model

To further analyze the impact of central heating on winter air pollution, we developed the linear regression model with the change of the adjusted AOD ratio as the dependent variable. The two datasets described above, the full dataset and the

one-obs-per-month-data-set, were used to fit the model. The independent variables include temperature during the heating season and population normalized central heating area. The spatial distribution of annual average values of parameters from 2003-2010 are shown in Figure 6, and the estimate of predictors in the model is shown in Table 4.

The spatial distribution of parameters are different (Figure 7). The distribution of the population normalized central heating area and temperature during the heating period is related to location: municipalities that are located in Northern China have lower average temperatures during the heating period and larger population normalized central heating area than municipalities that are located in Southern China. The normalized central heating area is also affected by municipalities' development: Beijing and Tianjin, the two major municipalities, have the highest value of the normalized central heating area.

Totally 2144 municipality-year in the all dataset and 2190 municipality-year in the one-obs-per-month dataset were used to fit the model. The collinearity issue was considered by the variance inflation factor (VIF). None of the parameters in the above two models have a VIF larger than 10; thus, collinearity is not an issue in these models.(Mason et al. 2003; Marquard.Dw 1970) The R^2 of the model based on the all dataset and one-obs-per-month dataset are 0.45 and 0.42, respectively. Thus, more

than 40% of the change of air pollution level during the heating period can be explained by our model. Both spatial and innerannual temperatures had significant negative relationships with the increase in air pollution level (p-value <0.05). A one degree decrease in interannual temperature was associated with a 0.059 unit increase of the adjusted AOD ratio in the heating period, and a one degree decrease in the spatial temperature was associated with a 0.085 unit increase of adjusted AOD ratio in the heating period. The interannual temperature and spatial temperature reflect the demand for heating. The lower the temperature is, the higher the demand for heating, and the higher the increase of air pollution level. The population normalized central heating area was significantly negatively related with the increase of the adjusted AOD ratio. A one-unit increase of population normalized central heating area led to an estimated 0.01~0.056 unit decrease in the change of the adjusted AOD ratio in the heating period. The spatial temperature and interannual temperature had a negative interaction with the population normalized central heating area. When the temperature in the heating period is held constant, the increase of the central heating area will decrease the air pollution level.

3.5 Spatiotemporal Variability of PM_{10}

To support the results from above analysis, that the air pollution level increases significantly during the heating period and this increase is significantly higher in the heating area relative to in the non-heating area, we also analyzed the ground measured

PM_{10} data from 2003-2012. PM_{10} is one of the three major ambient air pollutants regarded by the Chinese National Ambient Air Quality Standards(1996) and is treated as an indicator of PM pollution.(Pope 3rd 1989) The temporal variability of PM_{10} during each year from 2003-2012 is shown in Figure 8. The four spatiotemporal groups together with the entire study region during the study period described in section 3.2 were also used here. The annual PM_{10} concentration over the whole study area decreased from 109 $\mu g/m^3$ in 2003 to 86 $\mu g/m^3$ in 2010, with a decrease rate of 3.3 $\mu g/m^3$ per year. The average PM_{10} concentration in the heating area during the heating period decreased more sharply from 151 $\mu g/m^3$ in 2003 to 115 $\mu g/m^3$ in 2010, with a decrease rate of 5.1 $\mu g/m^3$. Nineteen per cent and four per cent of the total municipality-day during the heating and non-heating periods reported average PM_{10} concentrations exceeding the national standard (24-h average PM_{10} concentrations as 150 $\mu g/m^3$), respectively. The average PM_{10} concentration in the heating area during the heating period was always the highest among these spatiotemporal groups, with the average value from 2003 to 2010 being 126 $\mu g/m^3$, while that in the non-heating area during the non-heating period was always the lowest, with the average value from 2003 to 2010 being 64 $\mu g/m^3$. The average PM_{10} concentrations during the heating period are always higher than the corresponding values during the non-heating period. The increase of PM_{10} concentrations in the heating and non-heating areas was 38 and 24 $\mu g/m^3$, respectively.

Figure 9 shows the spatial distribution of long-term average PM_{10} concentration in heating and non-heating period from 2003-2010. The division of heating and non-heating period is the same as described before. The spatial distribution pattern of PM_{10} was similar to that of adjusted AOD. The average PM_{10} in the heating period in some areas in southern China, such as Yunnan, Fujian and Hainan province, were similar as those in the non-heating period; however, in other areas, the average PM_{10} concentration increased during the heating period. Paired t-test indicates that the average PM_{10} increases significantly by 31.9 $\mu g/m^3$ during the heating period (p-value<0.01).

To statistically analyze the impact of heating on the increase of PM_{10} concentrations in winter, several t-tests were conducted (Table 5). To eliminate the interannual variability, the PM_{10} concentration ratio was used in these tests. The t-test results indicate that the PM_{10} concentration increased significantly in winter (p-value<0.001) and the start of central heating significantly increase the PM_{10} concentration within two weeks (p-value<0.01).

3.6 Spatiotemporal Variability of $PM_{2.5}$ in 2013

To calibrate the analysis results of adjusted AOD, which is an indicator of ambient $PM_{2.5}$ concentration, we analyzed the ground measured $PM_{2.5}$ data in 2013. Because the continuous monitoring of $PM_{2.5}$ in China began at the end of 2012, we only have

one year entire year data of $PM_{2.5}$. The spatiotemporal pattern of $PM_{2.5}$ concentrations in 2013 in non-heating and heating periods were similar to those of adjusted AOD and PM_{10} (Figure 10), and most municipalities in Northern China reported higher $PM_{2.5}$ concentration during the heating period. Forty-eight per cent and eighteen per cent of the total city-day during the heating and non-heating periods reported average $PM_{2.5}$ concentrations exceeding the national $PM_{2.5}$ standard (24-h average as 75 $\mu g/m^3$), respectively. The paired t-test result indicates that the daily $PM_{2.5}$ concentrations increased by 46.2 $\mu g/m^3$ in the heating period (p-value<0.01).

4 Discussion

4.1 Spatiotemporal Variability of Air Pollution Levels

The average adjusted AOD and average PM_{10} concentrations for the heating area during the heating period were always higher than those for other spatiotemporal groups. This high air pollution level may be due to the meteorological factors and seasonal heating. The increase in the average adjusted AOD in the heating area during the heating period from 0.48 in 2003 to 0.85 in 2010 may have resulted from the increase in residents' ability to meet their heating demands and the increase in coal consumption for heating. Zhou et al. (2009) indicated that the per capita heating area in China increased from 7.14 to 16.17 m^2 from 1989-2005, and the per capita coal consumption for home heating correspondingly increased from 159.18 to 229.70 kg coal equivalent. From 2003-2010, the coal used for central heating increased from 85

to 167 million tonnes (Committee 2004, 2011). Previous analysis of the sources of $PM_{2.5}$ in Beijing using the positive matrix factorization (PMF) approach reported that the contribution of coal combustion to $PM_{2.5}$ concentration in the heating season increased from 37% to 57% from 2000-2009 (Song et al. 2006a; Song et al. 2006b; Zhang et al. 2013).

Our results show that the temporal trends of PM_{10} and adjusted AOD during the study period are very different (Figure 4 and Figure 8). The annual adjusted AOD in the entire study area keep approximately stable during this time period, while the corresponding annual PM_{10} concentrations decrease significantly. One explanation about this inconsistency could be that the size distribution of PM has changed in recent years. Adjusted AOD is highly related with $PM_{2.5}$ concentrations and the $PM_{2.5}/PM_{10}$ ratio may increase from 203-2010. However, previous studies do not support this explanation and report that the $PM_{2.5}/PM_{10}$ ratio keeps stable from 2003-2010. For example, in Beijing, the $PM_{2.5}/PM_{10}$ ratio ranged between 0.5-0.73 in 2001-2003 (Zhang et al. 2006; Sun et al. 2004), and the ratio was about 0.44 from 2009-2010 (Sun et al. 2011). In Nanjing, a city in Southern China, the $PM_{2.5}/PM_{10}$ ratio ranged between 0.54-0.84 in 2001, and the ratio was 0.73 recently (Wang et al. 2002; Shen et al. 2014). Another possible reason for this inconsistency is that the PM_{10} data was measured in cities, while the AOD data cover both the urban and rural

areas. Because there is no study about the possible difference of the $PM_{2.5}/PM_{10}$ ratio between urban and rural areas, further study is needed to support this hypothesis.

The t-test results indicate that the air pollution level responds to heating immediately. The air pollution level, indicated by the adjusted AOD value, the PM_{10} concentrations and the $PM_{2.5}$ concentrations, increases significantly in two weeks after heating start. The spatial and temporal distribution of adjusted AOD and $PM_{2.5}$ concentrations were similar: the highest values occur in Northeast China during heating periods. However, the spatial distribution of PM_{10} concentrations was different from the other two: the highest values occur in Shannxi and Shanxi provinces. This difference may be due to different sources of PM_{10} and $PM_{2.5}$: Shannxi and Shanxi provinces are located on the Loess Plateau and suffer from frequent sand storms, a natural source of PM that mainly affects PM_{10} concentrations. Thus the size distribution of PM in these two provinces may be different from in other areas. Previous studies reported that in Xi'an, the capital of Shannxi province, about 10% of the TSP with size <2.6 micron, while in Beijing, about 44% of the TSP was $PM_{2.5}$ (Sun et al. 2011; Cao et al. 2011).

4.2 Impact of Heating and Other Possible Air Pollution Sources

Based on the linear regression model, the increase in air pollution levels in the heating period is related to different factors, including temperature during the heating period, and the size of central heating area. Heating demands, indicated by the local

temperature, has a significant impact on the air pollution level. The lower the temperature during the heating season, the higher the heating demand, and leads to more heating activities and more pollution emission. When removing the two temperature indicators from the model, the R^2 will drop to 0.20 in the full dataset and to 0.16 in the one-obs-per-month dataset. Thus, temperature, or heating demands, can explain about 25% of the increase in the air pollution level in the heating period. The population normalized size of central heating area has a significant negative relationship with the increase in adjusted AOD ratio. This indicates that the central heating system has a pollution-control effect relative to other heating activities. People use different ways to meet their heating demands: in the municipalities in the heating area, residents may use the central heating system, while in areas where central heating is unavailable, such as in rural areas in Northern China and Southern China, residents may turn to domestic stoves and electric heating instruments. All these heating activities lead to air pollutant emission and increase the air pollution level. If the total heating demand is held the same and the more central heating is applied, then less individual heating is needed. Because the central heating system uses large-capacity boilers in heating stations and power plants to provide heat, it is more efficient relative to household operated stoves, and the centralized control of emissions is allowed. About 44% of the central heating is from the power plants and the capacity of the coal-fired power plants is 93% in the total thermal power plants in China (Xu et al. 2000; MoHaU-RDo China 2013). Coal-fired power plants with

capacities larger than 300MWe are required to install flue gas desulfurization (FGD) facilities by governmental regulation and this pollution-control action is estimated to reduce SO_2 emission by about 80% by 2010 (You and Xu 2010). Moreover, more than 96% of the coal-fired power plants installed electrostatic precipitators (ESP) facilities, which has a dust collection efficiency of more than 99% for TSP and more than 90% for $PM_{2.5}$ (You and Xu 2010; Zhao et al. 2008). Previous studies reported that the emission factor of PM for domestic coal combustion ranges between 1.3-19.6 g/kg, while the emission factor of PM for coal-fired power plants ranges between 0.4-2.0 g/kg when ESP was applied (Zhao et al. 2008; Zhao et al. 2010). Thus, central heating releases less air pollutant relative to individual heating and the higher percentage of central heating will lead to the lower air pollutant levels, holding total heating demand constant.

The intercept indicates a fixed increase in air pollution level in the heating period. This increase is believed to be associate with the change of meteorological factors: the heating period has a relatively slow wind speed and low boundary layer height (Yu et al. 2011).

4.3 Limitations and Future Study Directions

Due to snow/ice cover, there were some non-random missing data in Northern China during the heating period (Figure 2). To evaluate the potential bias due to the missing

data, two datasets were processed in this study: the full dataset and the one-obs-per-month dataset. The full dataset includes more MODIS pixels in Northern China, thus the increase rate of the adjusted AOD during the heating period is larger in this dataset relative to in the one-obs-per-month dataset (Table 2). Moreover, the full dataset provides more observations to develop the linear regression model and smaller p-values of predictors in the model. Because most of the non-random missing data occur during the heating-period, when the heating demand and the air pollution level are relatively high, this study may underestimate the increasing rate of the air pollution level in the heating period.

The relationship between AOD and $PM_{2.5}$ is a function of particle size distribution, composition, and vertical distribution, and may vary in different land use systems (Liu 2013; Tsai et al. 2011). In our study, we assumed that the relationship between AOD and $PM_{2.5}$ remains constant all year and we used the adjusted AOD ratio rather than the adjusted AOD value as target parameter to eliminate the impact of land use on the relationship between AOD and $PM_{2.5}$. Thus we analyzed the temporal variability of $PM_{2.5}$ concentration through analyzing the adjusted AOD ratio. The changes in aerosol composition, which may be due to unexpected events, such as forest fires, may also modify the relationship between AOD and $PM_{2.5}$ and bias this analysis. We assumed that there are no significant changes in aerosol composition in the study

period; however, detailed information about aerosol competition will help improve the accuracy of this analysis.

Due to the lack of detailed geographic and socioeconomic data, such as land use, motor vehicle number, and operation of local factories, we used the ratio of adjusted AOD to eliminate the spatial difference of the annual air pollution level and isolate the temporal increase of air pollution level in the heating period. Moreover, since the systematic monitoring of $PM_{2.5}$ began in 2012, we only have data on $PM_{2.5}$ concentrations for the entire year of 2013. $PM_{2.5}$ measurement data during a longer time period can help us develop the relationship between $PM_{2.5}$ and AOD. Together with detailed socioeconomic data, we can conduct a further analysis including more independent variables and provide more information for effective air pollution mitigation measures.

5 Conclusion

In this study, both the satellite retrieved data and ground measured air pollutant concentrations indicate that the air pollution levels increase significantly during the heating period and this increase is significantly higher in the heating areas than in the non-heating areas. The average adjusted AOD ratio and the PM_{10} concentrations ratio increased 2.78 and 0.33 in the heating period (p-value<0.01), respectively. In the heating area, the increase in the adjusted AOD ratio and PM_{10} ratio were higher than

those in the non-heating area by 2.19 (p-value<0.01) and 0.06 (p-value <0.01), respectively. Heating contributes significantly to the increase in air pollution levels during the heating period. The linear regression model indicates that central heating has significant pollution control effects relative to individual heating. Our findings further our understanding of winter air pollution in China and provide information for pollution-control policy making.

Acknowledgement

I would like to express my special appreciation and thanks to my thesis advisor, Dr. Liu, Yang, for the valuable guidance and advice. I would also like to thank Dr. Tolbert, Paige for serving as my committee member. I also want to thank faculty in the Environmental Health Department for attending my proposal presentation and providing comments. I would especially like to thank the Emory Environmental Remote Sensing Group for providing all the help and support when I conducted this project.

References

Pope CA, Dockery DW. 2006. Health effects of fine particulate air pollution: Lines that connect. J Air Waste Manage 56(6): 709-742.

Zhao JZ, Gao ZY, Tian ZY, Xie YQ, Xin F, Jiang RF, et al. 2013. The biological effects of individual-level PM2.5 exposure on systemic immunity and inflammatory response in traffic policemen. Occup Environ Med 70(6): 426-431.

Brook RD, Rajagopalan S, Pope CA, Brook JR, Bhatnagar A, Diez-Roux AV, et al. 2010. Particulate Matter Air Pollution and Cardiovascular Disease An Update to the Scientific Statement From the American Heart Association. Circulation 121(21): 2331-2378.

Vineis P, Hoek G, Krzyzanowski M, Vigna-Taglianti F, Veglia F, Airoldi L, et al. 2006. Air pollution and risk of lung cancer in a prospective study in Europe. Int J Cancer 119(1): 169-174.

Franklin M, Zeka A, Schwartz J. 2007. Association between PM2.5 and all-cause and specific-cause mortality in 27 US communities. J Expo Sci Env Epid 17(3): 279-287.

Pope CA, 3rd, Ezzati M, Dockery DW. 2009. Fine-particulate air pollution and life expectancy in the United States. The New England journal of medicine 360(4): 376-386.

Kan HD, London SJ, Chen GH, Zhang YH, Song GX, Zhao NQ, et al. 2007. Differentiating the effects of fine and coarse particles on daily mortality in Shanghai, China. Environment international 33(3): 376-384.

Kappos AD, Bruckmann P, Eikmann T, Englert N, Heinrich U, Hoppe P, et al. 2004. Health effects of particles in ambient air. Int J Hyg Envir Heal 207(4): 399-407.

Bell ML, Samet JM, Dominici F. 2004. Time-series studies of particulate matter. Annu Rev Publ Health 25: 247-280.

Organization WH. 2006. WHO Air quality guidelines for particulate matter, ozone, nitrogen dioxide and sulfur dioxide. Switzerland: WHO Press.

China MoEPo. 2013. National Ambient Air Quality Standards for Particulate Matter. HJ 633-2012.

China MoEPo. 2012. Technical Regulation on Ambient Air Quality Index.

Cao JJ, Lee SC, Chow JC, Watson JG, Ho KF, Zhang RJ, et al. 2007. Spatial and seasonal distributions of carbonaceous aerosols over China. J Geophys Res-Atmos 112(D22).

Zhao PS, Dong F, He D, Zhao XJ, Zhang XL, Zhang WZ, et al. 2013. Characteristics of concentrations and chemical compositions for PM2.5 in the region of Beijing, Tianjin, and Hebei, China. Atmos Chem Phys 13(9): 4631-4644.

He KB, Yang FM, Ma YL, Zhang Q, Yao XH, Chan CK, et al. 2001. The characteristics of PM2.5 in Beijing, China. Atmos Environ 35(29): 4959-4970.

Zhou ZR, Wu WL, Wang XH, Chen Q, Wang O. 2009. Analysis of changes in the structure of rural household energy consumption in northern China: A case study. Renew Sust Energ Rev 13(1): 187-193.

Cai WG, Wu Y, Zhong Y, Ren H. 2009. China building energy consumption: Situation, challenges and corresponding measures. Energ Policy 37(6): 2054-2059.

Committee CEPYE. 2004. China Electric Power Yearbook. China.

Chen Y, Sheng G, Bi X, Feng Y, Mai B, Fu J. 2005. Emission factors for carbonaceous particles and polycyclic aromatic hydrocarbons from residential coal combustion in China. Environmental science & technology 39(6): 1861-1867.

Song Y, Xie SD, Zhang YH, Zeng LM, Salmon LG, Zheng M. 2006a. Source apportionment of PM2.5 in Beijing using principal component analysis/absolute principal component scores and UNMIX. Science of the Total Environment 372(1): 278-286.

Song Y, Zhang YH, Xie SD, Zeng LM, Zheng M, Salmon LG, et al. 2006b. Source apportionment of PM2.5 in Beijing by positive matrix factorization. Atmos Environ 40(8): 1526-1537.

Zhang R, Jing J, Tao J, Hsu SC, Wang G, Cao J, et al. 2013. Chemical characterization and source apportionment of PM2.5 in Beijing: seasonal perspective. Atmos Chem Phys 13(14): 7053-7074.

Chen Y, Ebenstein A, Greenstone M, Li H. 2013. Evidence on the impact of sustained exposure to air pollution on life expectancy from China's Huai River policy. Proceedings of the National Academy of Sciences of the United States of America 110(32): 12936-12941.

Liu Y, He K, Li S, Wang Z, Christiani DC, Koutrakis P. 2012. A statistical model to evaluate the effectiveness of PM2.5 emissions control during the Beijing 2008 Olympic Games. Environment international 44: 100-105.

Hu XF, Waller LA, Al-Hamdan MZ, Crosson WL, Estes MG, Estes SM, et al. 2013. Estimating ground-level PM2.5 concentrations in the southeastern US using geographically weighted regression. Environ Res 121: 1-10.

Liu Y. 2013. New Directions: Satellite driven PM2.5 exposure models to support targeted particle pollution health effects research. Atmos Environ 68: 52-53.

Song C-K, Ho C-H, Park RJ, Choi Y-S, Kim J, Gong D-Y, et al. 2009. Spatial and seasonal variations of surface PM10 concentration and MODIS aerosol optical depth over China. Asia-Pacific Journal of Atmospheric Sciences 45(1): 33-43.

Wang LL, Xin JY, Wang YS, Li ZQ, Liu GR, Li J. 2007. Evaluation of the MODIS aerosol optical depth retrieval over different ecosystems in China during EAST-AIRE. Atmos Environ 41(33): 7138-7149.

Wang LL, Wang YS, Xin JY, Li ZQ, Wang XY. 2010. Assessment and comparison of three years of Terra and Aqua MODIS Aerosol Optical Depth Retrieval (C005) in Chinese terrestrial regions. Atmos Res 97(1-2): 229-240.

Tsai TC, Jeng YJ, Chu DA, Chen JP, Chang SC. 2011. Analysis of the relationship between MODIS aerosol optical depth and particulate matter from 2006 to 2008. Atmos Environ 45(27): 4777-4788.

Hubanks PA, King MD, Platnick S, Pincus R. 2008. MODIS atmosphere L3 gridded product algorithm theoretical basis document. Algorithm Theor Basis Doc ATBD-MOD 30.

Ruiz-Arias JA, Dudhia J, Gueymard CA, Pozo-Vazquez D. 2013. Assessment of the Level-3 MODIS daily aerosol optical depth in the context of surface solar radiation and numerical weather modeling. Atmos Chem Phys 13(2): 675-692.

Dawson J, Adams P, Pandis S. 2007. Sensitivity of PM 2.5 to climate in the eastern US: A modeling case study. Atmos Chem Phys 7(16): 4295-4309.

Alfoldy B, Osan J, Toth Z, Torok S, Harbusch A, Jahn C, et al. 2007. Aerosol optical depth, aerosol composition and air pollution during summer and winter conditions in Budapest. The Science of the total environment 383(1-3): 141-163.

Koelemeijer R, Homan C, Matthijsen J. 2006. Comparison of spatial and temporal variations of aerosol optical thickness and particulate matter over Europe. Atmos Environ 40(27): 5304-5315.

Gong DY, Ho CH, Chen DL, Qian Y, Choi YS, Kim JW. 2007. Weekly cycle of aerosol-meteorology interaction over China. J Geophys Res-Atmos 112(D22).

Choi YS, Ho CH, Chen D, Noh YH, Song CK. 2008. Spectral analysis of weekly variation in PM10 mass concentration and meteorological conditions over China. Atmos Environ 42(4): 655-666.

Dobson JE, Bright EA, Coleman PR, Durfee RC, Worley BA. 2000. LandScan: a global population database for estimating populations at risk. Photogrammetric engineering and remote sensing 66(7): 849-857.

Zhang W, Sun Y, Zhuang G, Xu D. 2006. Characteristics and seasonal variations of PM2. 5, PM10, and TSP aerosol in Beijing. Biomedical and Environmental Sciences 19(6): 461.

Mason RL, Gunst RF, Hess JL. 2003. Statistical design and analysis of experiments: with applications to engineering and science: John Wiley & Sons.

Marquard.Dw. 1970. Generalized Inverses, Ridge Regression, Biased Linear Estimation, and Nonlinear Estimation. Technometrics 12(3): 591-&.

[Anonymous]. 1996. Chinese National Ambient Air Quality Standard. GB3095-1996.

Pope 3rd C. 1989. Respiratory disease associated with community air pollution and a steel mill, Utah Valley. American Journal of Public Health 79(5): 623-628.

Committee CEPYE. 2011. China Electric Power Yearbook China Electric Power Press.

Sun Y, Zhuang G, Wang Y, Han L, Guo J, Dan M, et al. 2004. The air-borne particulate pollution in Beijing—concentration, composition, distribution and sources. Atmos Environ 38(35): 5991-6004.

Sun Y, Pan Y, Li X, Zhu R, Wang Y. 2011. [Chemical composition and mass closure of particulate matter in Beijing, Tianjin and Hebei megacities, Northern China]. Huan jing ke xue= Huanjing kexue/[bian ji, Zhongguo ke xue yuan huan jing ke xue wei yuan hui" Huan jing ke xue" bian ji wei yuan hui] 32(9): 2732-2740.

Wang G, Huang L, Gao S, Gao S, Wang L. 2002. Measurements of PM10 and PM2. 5 in urban area of Nanjing, China and the assessment of pulmonary deposition of particle mass. Chemosphere 48(7): 689-695.

Shen GF, Yuan SY, Xie YN, Xia SJ, Li L, Yao YK, et al. 2014. Ambient levels and temporal variations of PM2. 5 and PM10 at a residential site in the mega-city, Nanjing, in the western Yangtze River Delta, China. Journal of Environmental Science and Health, Part A 49(2): 171-178.

Cao Z, Yang Y, Lu J, Zhang C. 2011. Atmospheric particle characterization, distribution, and deposition in Xi'an, Shaanxi Province, Central China. Environ Pollut 159(2): 577-584.

Xu X, Chen C, Qi H, He R, You C, Xiang G. 2000. Development of coal combustion pollution control for SO< sub> 2</sub> and NO< sub> x</sub> in China. Fuel Processing Technology 62(2): 153-160.

China MoHaU-RDo. 2013. China's urban construction statistical yearbook 2012. China Plans to Press.

You CF, Xu XC. 2010. Coal combustion and its pollution control in China. Energy 35(11): 4467-4472.

Zhao Y, Wang SX, Duan L, Lei Y, Cao PF, Hao JM. 2008. Primary air pollutant emissions of coal-fired power plants in China: Current status and future prediction. Atmos Environ 42(36): 8442-8452.

Zhao Y, Wang S, Nielsen CP, Li X, Hao J. 2010. Establishment of a database of emission factors for atmospheric pollutants from Chinese coal-fired power plants. Atmos Environ 44(12): 1515-1523.

Yu Y, Schleicher N, Norra S, Fricker M, Dietze V, Kaminski U, et al. 2011. Dynamics and origin of PM2.5 during a three-year sampling period in Beijing, China. J Environ Monitor 13(2): 334-346.

Zheng M, Salmon LG, Schauer JJ, Zeng LM, Kiang CS, Zhang YH, et al. 2005. Seasonal trends in PM2.5 source contributions in Beijing, China. Atmos Environ 39(22): 3967-3976.

Duan FK, He KB, Ma YL, Yang FM, Yu XC, Cadle SH, et al. 2006. Concentration and chemical characteristics of PM2.5 in Beijing, China: 2001-2002. Science of the Total Environment 355(1-3): 264-275.

Geng NB, Wang J, Xu YF, Zhang WD, Chen C, Zhang RQ. 2013. PM2.5 in an industrial district of Zhengzhou, China: Chemical composition and source apportionment. Particuology 11(1): 99-109.

Yang LX, Zhou XH, Wang Z, Zhou Y, Cheng SH, Xu PJ, et al. 2012. Airborne fine particulate pollution in Jinan, China: Concentrations, chemical compositions and influence on visibility impairment. Atmos Environ 55: 506-514.

Ye BM, Ji XL, Yang HZ, Yao XH, Chan CK, Cadle SH, et al. 2003. Concentration and chemical composition of PM2.5 in Shanghai for a 1-year period. Atmos Environ 37(4): 499-510.

Tian YZ, Wu JH, Shi GL, Wu JY, Zhang YF, Zhou LD, et al. 2013. Long-term variation of the levels, compositions and sources of size-resolved particulate matter in a megacity in China. Science of the Total Environment 463: 462-468.

Xu LL, Chen XQ, Chen JS, Zhang FW, He C, Zhao JP, et al. 2012. Seasonal variations and chemical compositions of PM2.5 aerosol in the urban area of Fuzhou, China. Atmos Res 104: 264-272.

Zhang FW, Xu LL, Chen JS, Yu YK, Niu ZC, Yin LQ. 2012. Chemical compositions and extinction coefficients of PM2.5 in peri-urban of Xiamen, China, during June 2009-May 2010. Atmos Res 106: 150-158.

Chang SC, Chou CCK, Chan CC, Lee CT. 2010. Temporal characteristics from continuous measurements of PM2.5 and speciation at the Taipei Aerosol Supersite from 2002 to 2008. Atmos Environ 44(8): 1088-1096.

Tables and Figures

Table 1 Previous monitoring results about $PM_{2.5}$ concentrations in China

City	24-h PM2.5 Concentrations μg/m3					Reference
	Annual	Spring	Summer	Fall	Winter	
Beijing	121	89.0	76.0	112	176	He et al. (2001)
Beijing	101	139	99.0	106	60.9	Zheng et al. (2005)
Beijing	102	76.4	89.0	79.8	122	Duan et al. (2006)
Beijing	64.4	76.5	60.9	63.2	74.5	Yu et al. (2011)
Beijing	123	128	116	124	127	PS Zhao et al. (2013)
Tianjin	142	136	161	152	117	
Shijiazhuang	191	175	146	219	227	
Chengdu	92.4	105	67.8	74.4	123	
Zhengzhou	175	181	122	186	211	Geng et al. (2013)
Jinan	149	143	129	135	205	Yang et al. (2012)
Shanghai	57.9	61.7	36.8	64.8	88.6	Ye et al. (2003)
Chengdu	165±85.1	133	114	188	226	Tian et al. (2013)
Fuzhou	44.3±16.3	49.8	23.6	44.1	59.8	Xu et al. (2012)

Xiamen	86.2	89.7	62.3	83.8	109	Zhang et al. (2012)
Taipei	30.3±16.0	34.5	26.7	27.0	32.8	Chang et al. (2010)

Table 2 Summary statistics of meteorological and social-economic parameters

Variable	**Mean**	**Std. Dev.**	**Min**	**Max**
Municipality-level Adjusted AOD Ratio Difference (full)	2.32	1.68	-0.76	23.7
Municipality-level Adjusted AOD Ratio Difference (one-obs-per-month)	1.73	0.82	-0.78	5.74
Interannual Temperature ℃	0	1.18	-4.89	3.56
Spatial Temperature ℃	3.62	7.88	-19.2	22.1
Population Normalized Central Heating Area $km^2/10^4$ persons	2.47	3.79	0	32.2

Table 3 T-test results of adjusted AOD

T-test	**Difference**	
	Full dataset	One-obs-per-month dataset
AOD ratio during heating period	2.30 ***	1.72 ***

and non-heating period		
AOD ratio before and after heating start	1.36 ***	1.11 ***
Increase of adjusted AOD ratio in heating period between the heating and non-heating areas	1.44 ***	0.94 ***

*** P-value<0.01

Table 4 Estimates of parameters in the linear regression models

Variable	**Full dataset N=2344 R^2=0.45**	**One-obs-per-month dataset N=2190 R^2=0.42**
Intercept	2.6***	2.1***
Interannual Temperature	-0.059**	-0.031**
Spatial Temperature	-0.098***	-0.075***
Population normalized Central Heating Area	-0.056***	-0.010*
Central Heat ×Interannual Temperature	-0.022***	0.0018
Central Heating ×Spatial Temperature	-0.020***	-0.0018*

*p-value< 0.1

**p-value< 0.05

***p-value< 0.01

Table 5 The t-test results of PM_{10} concentrations

T-test	Difference
PM_{10} ratio during heating period and non-heating period	0.35***
PM_{10} ratio before and after heating start	0.20***
Increase of PM_{10} ratio in heating period in the heating and non-heating areas	0.007

***p-value< 0.01

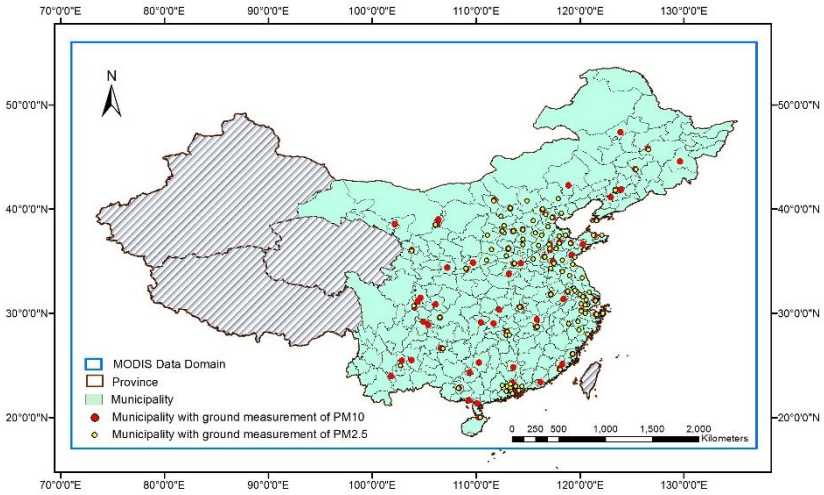

Figure 1 Study region. The western provinces (Xinjiang, Qinghai, and Tibet) were excluded. The red dots represent cities with ground PM_{10} monitors and the yellow dots represent cities with ground $PM_{2.5}$ monitors.

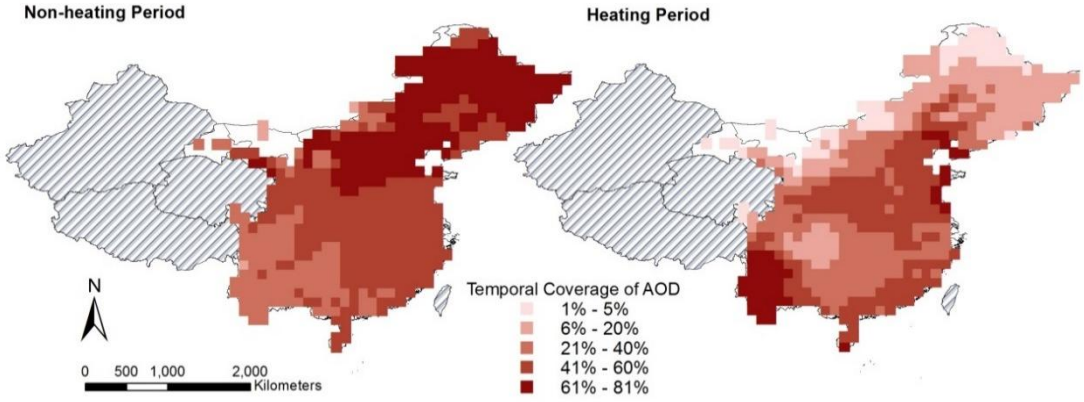

Figure 2 Temporal coverage of AOD data in the heating and non-heating periods.

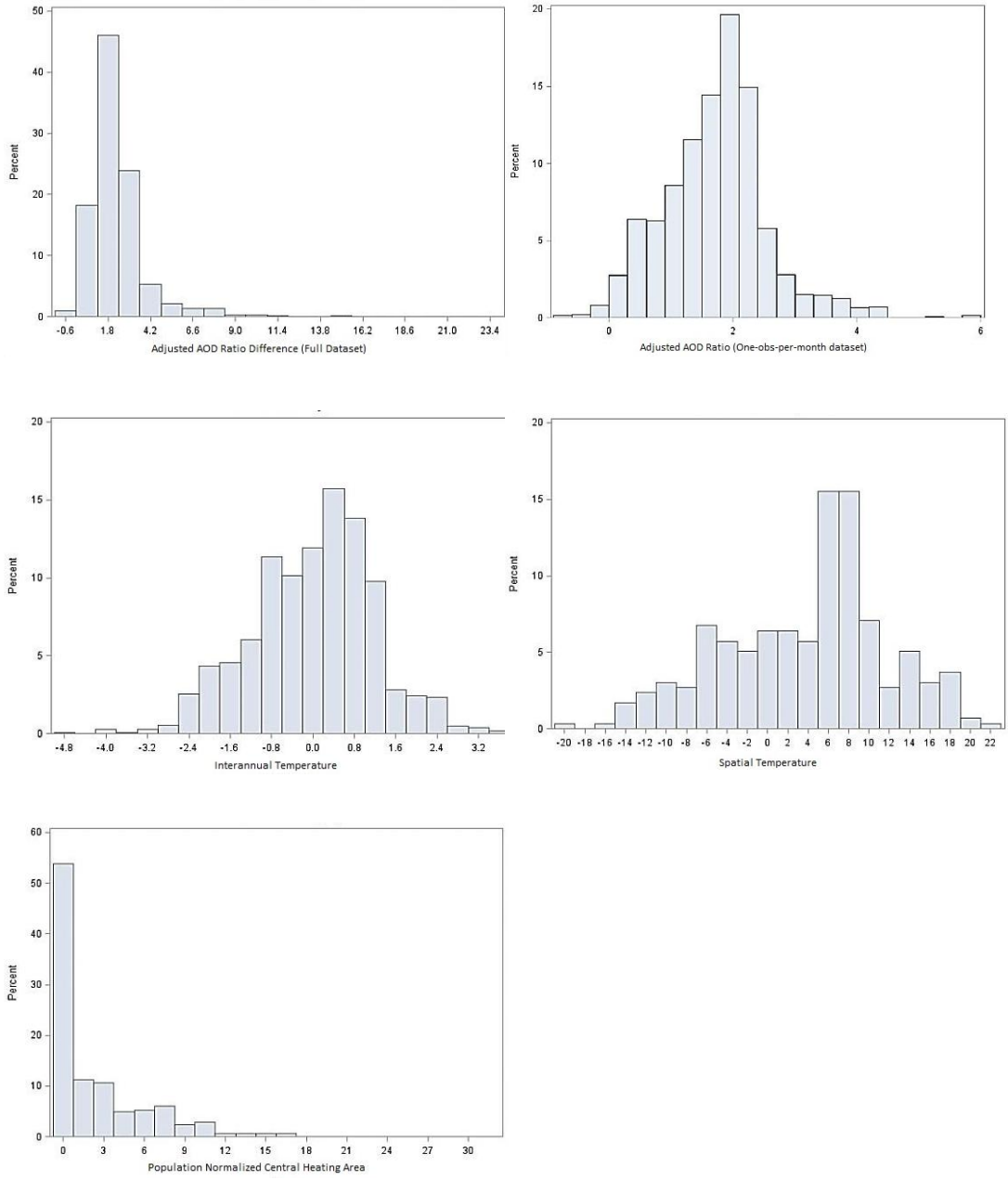

Figure 3 Histograms of dependent and independent variables.

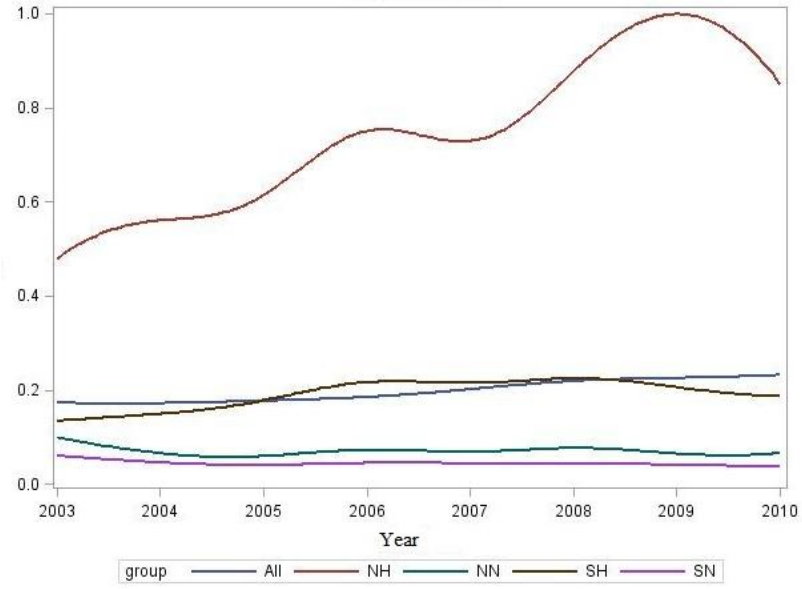

Figure 4 Average AOD in heating/non-heating periods in heating and non-heating areas in China All, Annual average AOD over the entire study region HH, in the heating area during the heating period HN, in the heating area during the non-heating period NH, in the non-heating area during the heating period NN, in the non-heating area during the non-heating period. Data of this figure was from the full dataset.

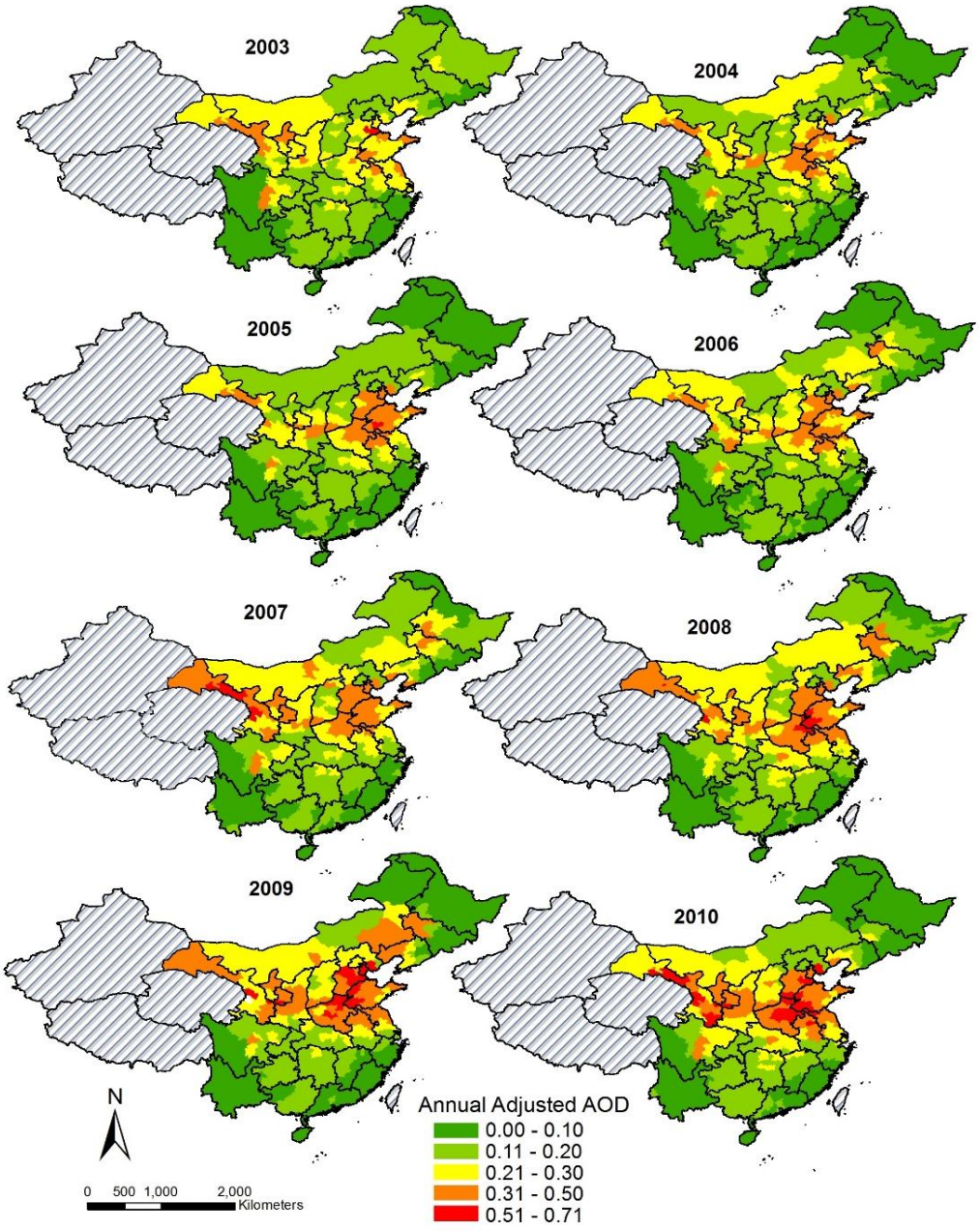

Figure 5 Spatial distribution of annual adjusted AOD from 2003-2010.

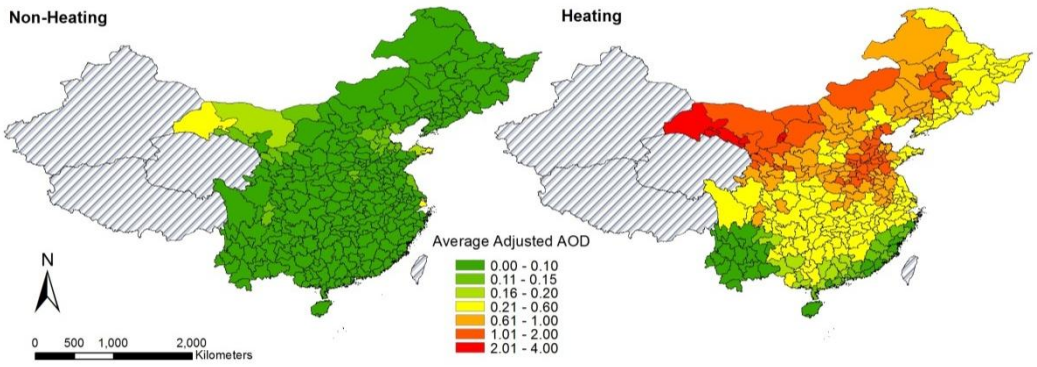

Figure 6 Spatial distribution of eight-year-average adjusted AOD during the heating and non-heating periods.

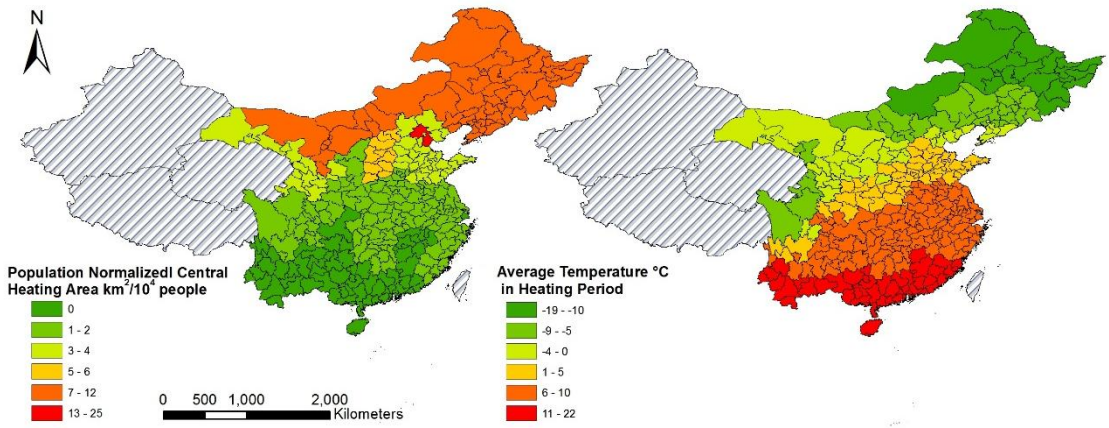

Figure 7 Spatial distribution of population normalized central heating area and spatial temperature in China.

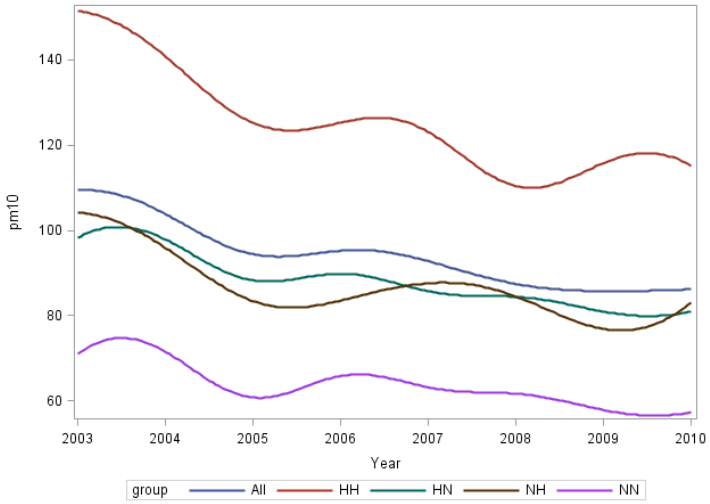

Figure 8 Average PM_{10} concentrations in heating/non-heating periods in heating/non-heating areas in China All, Annual average PM_{10} over the entire study region HH, average PM_{10} in the heating area during the heating period HN, average PM_{10} in the heating area during the non-heating period NH, average PM_{10} in the non-heating area during the heating period NN, average PM_{10} in the non-heating area during the non-heating period.

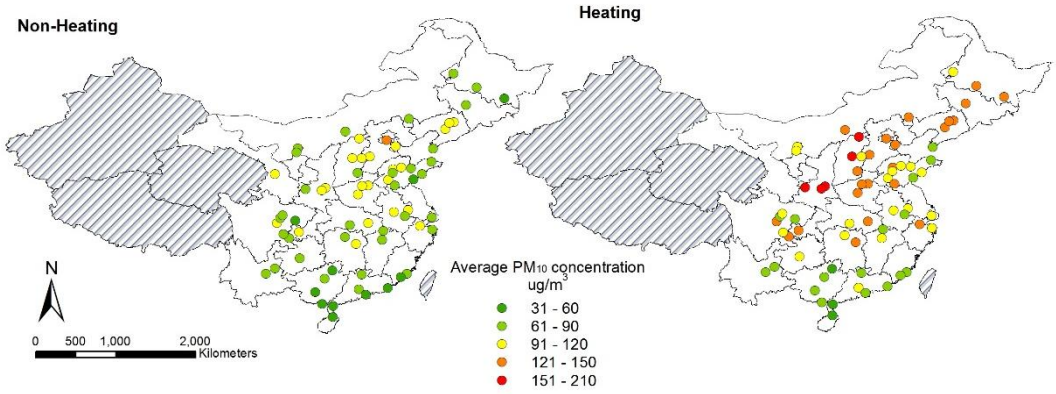

Figure 9 Average PM_{10} concentrations from 2003-2010 in heating and non-heating period.

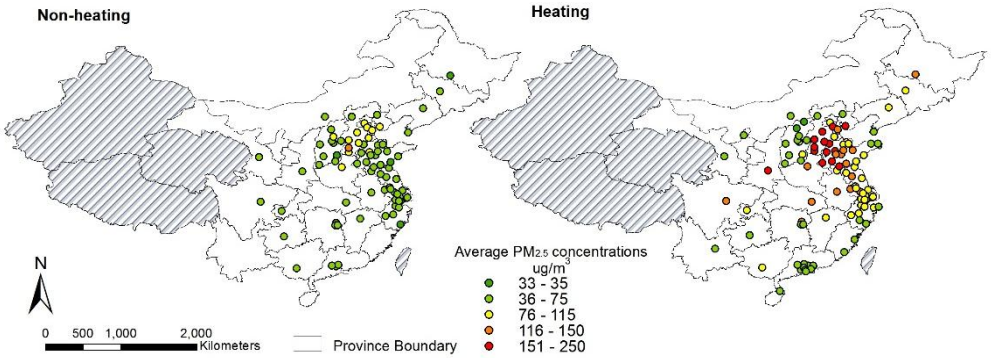

Figure 10 Average $PM_{2.5}$ concentrations in 2013 in heating and non-heating period.